Annals of Nuclear Energy 37 (2010) 1214–1222

Contents lists available at ScienceDirect

Annals of Nuclear Energy

journal homepage: www.elsevier.com/locate/anucene

Subcritical multiplication factor and source efficiency in accelerator-driven system

Hesham Shahbunder [a,*], Cheol Ho Pyeon [b], Tsuyoshi Misawa [b], Jae-Yong Lim [b], Seiji Shiroya [b]

[a] Department of Fundamental Energy Science, Graduate School of Energy Science, Kyoto University, Yoshida-honmachi, Sakyo-ku, Kyoto 606-8501, Japan
[b] Nuclear Engineering Science Division, Research Reactor Institute, Kyoto University, Asashiro-nishi, Kumatori-cho, Sennan-gun, Osaka 590-0494, Japan

ARTICLE INFO

Article history:
Received 16 February 2010
Received in revised form 9 April 2010
Accepted 17 April 2010
Available online 26 May 2010

Keywords:
ADS
KUCA
Reaction rate distribution
Subcritical multiplication factor
Neutron source efficiency
MCNPX

ABSTRACT

The subcritical multiplication factor k_s and the external neutron source efficiency φ^* are important parameters in the accelerator-driven system (ADS) performance assessment. The theoretical relation between k_s and the effective multiplication factor k_{eff} in a subcritical system is discussed in different cases of subcritical system. On the basis of the theoretical background, the dependence of k_s and φ^* on subcriticality, source position, and energy is numerically investigated using a simple thermal subcritical model. For the sake of experimental evaluation of k_s and φ^*, the ADS experiments have been carried out in the subcritical systems combined with 14 MeV pulsed neutrons of the Kyoto University Critical Assembly (KUCA). The k_s and φ^* parameters are successfully measured by utilizing the reaction rate distribution obtained by the optical fiber detectors in the subcritical system, within a relative difference of less than 7% and 12% for k_s and φ^*, respectively, between measured and calculated values for most studied cases.

1. Introduction

The accelerator-driven system (ADS) is being developed for energy production, transmutation of spent fuel and usage as a neutron source (Carminati et al., 1993; Takahashi, 1994; Delpech et al., 1999). The basic ADS experimental investigations were carried out in the "Yalina" subcritical assembly facility, coupled to D–D or D–T sources (Persson et al., 2005, 2008; Kiyavitskaya, 2007), and the Kyoto University Critical Assembly "KUCA" facility coupled to D–T source (Pyeon et al., 2007, 2008, 2009a; Shiroya et al., 2000; Misawa and Unesaki, 2003; Shahbunder et al., 2010). These investigations were aimed to study the nuclear characteristics in reactor physics and examine the neutronic properties of ADS. The study of ADS in KUCA was extended by using the Fixed Field Alternating Gradient (FFAG) accelerator (Tanigaki et al., 2006). The protons beam (100 MeV) generated by the FFAG accelerator were recently successfully injected onto a tungsten target in the KUCA polyethylene moderated- and reflected-core (A-core) (Pyeon et al., 2009b).

ADS is intended to operate at sufficiently deep subcriticality level to maintain the over-all safety. While subcriticality is an important concept for monitoring the safety of reactor operation in critical or very close to critical states, a new definition of subcriticality is of the same importance in ADS, if it could be used to optimize the reactor size and power for extended periods of operation. The effective multiplication factor k_{eff}, obtained by solving the neutron balance equation, is usually employed to express the subcriticality. However, k_{eff} parameter doesn't consider the effect of the source position and/or energy. Another parameter that is the subcritical multiplication factor k_s was then introduced to express the subcriticality for the ADS reactors (Kobayashi and Nishihara, 2000; Gandini and Salvatores, 2002; Nishihara et al., 2003). The k_s is defined as the ratio of the fission neutrons to the total neutrons in the system by fission and source. It is directly related to the neutron multiplication M (Shi et al., 2005) as follows:

$$M = \frac{1}{1 - k_s}. \quad (1)$$

The neutron source efficiency φ^* (Salvatores, 1999) was introduced as another parameter relating k_s to the conventional k_{eff} of the system. The source efficiency φ^* was an index of the source importance relative to the fission and how much it could contribute to the final fission events and the total power of the system.

The k_s and φ^* parameters were commonly used in the physics of ADS, since they played an important role in the ADS performance assessment (Gandini and Salvatores, 2002; Seltborg et al., 2003; Seltborg and Jacqmin, 2001b; Shi et al., 2005). For instance, the total reactor power P in the subcritical system, which is simply derived from the product of the fission rate and the energy released per fission, can be expressed by using k_s as follows (Heuer et al., 1997):

* Corresponding author. Tel.: +81 72 451 2359; fax: +81 72 451 2603.
E-mail address: hesham@rri.kyoto-u.ac.jp (H. Shahbunder).

0306-4549/$ - see front matter © 2010 Elsevier Ltd. All rights reserved.
doi:10.1016/j.anucene.2010.04.010

$$P = \left(\frac{P_{beam}}{\varepsilon_n}\right)\left(\frac{k_s}{\nu(1-k_s)}\right)\varepsilon_f, \quad (2)$$

where P_{beam} is the beam power, ε_n and ε_f are the energies consumed and released per source neutron production and nuclear fission, respectively, and ν is the average neutrons released per fission. The k_s should be monitored to confirm that it remains constant over a given period of operation to provide, in turn, sufficiently constant power which is desirable especially for the power reactors. If k_{eff} in the subcritical system is known, k_s can be used to obtain φ^*. From the relation between k_s and k_{eff}, the total reactor power in Eq. (2) can be expressed by using the source efficiency φ^* as follows:

$$P = \left(\frac{P_{beam}}{\varepsilon_n}\right)\left(\frac{\varphi^* k_{eff}}{\nu(1-k_{eff})}\right)\varepsilon_f. \quad (3)$$

As seen in Eq. (3), an optimization of the source in the system to accomplish higher φ^* can reduce the beam current and power requirements for a given subcritical state, and thus the system becomes more efficient.

The k_s concept in this study was theoretically discussed to clarify the relation between the multiplication factors k_s and k_{eff} in subcritical system. In addition, a simple subcritical model was introduced to numerically investigate the effect of subcriticality, source position and energy on k_s and φ^*.

In the previous study (Shahbunder et al., 2010), an experimental methodology was confirmed to successfully evaluate the neutron multiplication M using the measured reaction rate distribution in the subcritical systems. On the basis of the same methodology, the present study was extended to examine an experimental evaluation of k_s and φ^* using the measured reaction rate distribution in the ADS experiments with 14 MeV neutrons carried out at the KUCA A-core.

2. Subcritical multiplication factor and source efficiency

The neutron balance equation in fundamental mode is expressed as follows:

$$\mathbf{L}\phi_0(\mathbf{r},E) = \frac{1}{k_{eff}}\mathbf{P}\phi_0(\mathbf{r},E), \quad (4)$$

where $\phi_0(\mathbf{r},E)$ is the neutron flux distribution at position $\mathbf{r}(x,y,z)$ with energy E, k_{eff} is the effective multiplication factor, and $\mathbf{L}$ and $\mathbf{P}$ are the destruction and production operators, respectively. By taking the inner product $\langle .,. \rangle$ of Eq. (4), which indicates the integration over the space and energy variables, k_{eff} in Eq. (4) can be expressed as follows:

$$k_{eff} = \frac{\langle \mathbf{P}\phi_0(\mathbf{r},E)\rangle}{\langle \mathbf{L}\phi_0(\mathbf{r},E)\rangle}. \quad (5)$$

From Eq. (5), the multiplication factor of a system can be understood as "the number of fission neutrons produced per lost neutrons." This concept can be applied to subcritical systems with an external source as shown in next section.

2.1. Subcritical multiplication factor k_s

The neutron balance equation describing a subcritical system with an external source at steady state is given as follows:

$$\mathbf{L}\phi_s(\mathbf{r},E) = \mathbf{P}\phi_s(\mathbf{r},E) + s(\mathbf{r},E), \quad (6)$$

where $\phi_s(\mathbf{r},E)$ is the neutron flux in this subcritical system with the existence of the external neutron source $s(\mathbf{r},E)$.

By applying the concept of the multiplication factor to the subcritical system in Eq. (6), the *subcritical multiplication factor* k_s can be expressed as follows:

$$k_s = \frac{\langle \mathbf{P}\phi_s(\mathbf{r},E)\rangle}{\langle \mathbf{L}\phi_s(\mathbf{r},E)\rangle}. \quad (7)$$

By integrating Eq. (6) over space and energy, and substituting in Eq. (7), k_s can be expressed as follows:

$$k_s = \frac{\langle \mathbf{P}\phi_s(\mathbf{r},E)\rangle}{\langle \mathbf{P}\phi_s(\mathbf{r},E)\rangle + \langle s(\mathbf{r},E)\rangle} = \frac{F}{F+S}, \quad (8)$$

$$F \equiv \int_V \int_0^\infty \nu\Sigma_f(\mathbf{r},E)\phi_s(\mathbf{r},E)\,dE\,d^3r, \quad (9)$$

$$S \equiv \int_V \int_0^\infty s(\mathbf{r},E)\,dE\,d^3r, \quad (10)$$

where F is the total fission neutrons, S is the total source neutrons, V is the whole system volume, ν is the average number of fission neutrons per fission reaction, and $\Sigma_f(\mathbf{r},E)$ is the fission cross-section.

The concept of k_s for subcritical system in steady state with external source is equivalent to that of k_{eff} for the critical system in steady state, since they both can describe the number of fission neutrons produced per lost neutron in the corresponding system.

2.2. Relationship between k_s and k_{eff} in subcritical system

For the subcritical system in steady state which is very close to the critical state, the relative neutron flux distribution ϕ_s is approximately equal to that of the critical system ϕ_0 and therefore the value of k_s could become approximately as same as that of k_{eff}.

On the other hand, for a deeper subcritical system in steady state, the relative neutron flux distribution of ϕ_s in Eq. (6) is considerably different from that of ϕ_0 in Eq. (4). This means that k_{eff} in the deeper subcritical case is not produced by the actual neutron flux ϕ_s of the system but rather by an "imaginary" neutron flux ϕ_0. The imaginary system expressed by ϕ_0 can satisfy the homogenous equation in the critical system, if the average neutrons per fission reaction is assumed to be ν/k_{eff} (Duderstadt and Hamilton, 1976) rather than only ν as in the normal condition. Here, by taking the adjoint flux and operators of both sides of Eq. (4), multiplying from the left by $\phi_s(\mathbf{r},E)$, and integrating over-all space and energy, the following equation can be obtained:

$$\langle \phi_s(\mathbf{r},E), \mathbf{L}^\dagger\phi_0^\dagger(\mathbf{r},E)\rangle = \frac{1}{k_{eff}}\langle \phi_s(\mathbf{r},E), \mathbf{P}^\dagger\phi_0^\dagger(\mathbf{r},E)\rangle. \quad (11)$$

From the properties of the adjoint operator, Eq. (11) can be rewritten after rearranging as follows:

$$\frac{\langle \phi_0^\dagger(\mathbf{r},E), \mathbf{L}\phi_s(\mathbf{r},E)\rangle}{\langle \phi_0^\dagger(\mathbf{r},E), \mathbf{P}\phi_s(\mathbf{r},E)\rangle} = \frac{1}{k_{eff}}. \quad (12)$$

On the other side, by multiplying Eq. (6) to the adjoint neutron flux $\phi_0^\dagger$ from the left, and integrating, the following equation can be obtained:

$$\langle \phi_0^\dagger(\mathbf{r},E), \mathbf{L}\phi_s(\mathbf{r},E)\rangle = \langle \phi_0^\dagger(\mathbf{r},E), \mathbf{P}\phi_s(\mathbf{r},E)\rangle + \langle \phi_0^\dagger(\mathbf{r},E), s(\mathbf{r},E)\rangle. \quad (13)$$

By dividing Eq. (13) by $\langle \phi_0^\dagger(\mathbf{r},E), \mathbf{P}\phi_s(\mathbf{r},E)\rangle$, the following equation can be obtained:

$$\frac{\langle \phi_0^\dagger(\mathbf{r},E), \mathbf{L}\phi_s(\mathbf{r},E)\rangle}{\langle \phi_0^\dagger(\mathbf{r},E), \mathbf{P}\phi_s(\mathbf{r},E)\rangle} = 1 + \frac{\langle \phi_0^\dagger(\mathbf{r},E), s(\mathbf{r},E)\rangle}{\langle \phi_0^\dagger(\mathbf{r},E), \mathbf{P}\phi_s(\mathbf{r},E)\rangle}. \quad (14)$$

Here, the *external source efficiency* φ^* (Salvatores, 1999) is introduced and defined as follows:

$$\varphi^* \equiv \frac{\langle \phi_0^\dagger(\mathbf{r},E), s(\mathbf{r},E)\rangle}{\langle s(\mathbf{r},E)\rangle} \Big/ \frac{\langle \phi_0^\dagger(\mathbf{r},E), \mathbf{P}\phi_s(\mathbf{r},E)\rangle}{\langle \mathbf{P}\phi_s(\mathbf{r},E)\rangle}. \quad (15)$$

As seen in Eq. (15), the external source efficiency φ^* represents the ratio of the average external source importance (numerator) to the average fission importance (denominator). This representation implies the efficiency of the external neutron source, with a certain position and energy configuration, in producing "important" neutrons which are desirable for higher neutron multiplication and power level for a given subcritical system. By using definition of φ^* in Eq. (15), Eq. (14) can be expressed as follows:

$$\frac{\langle \phi_0^\dagger(\mathbf{r},E), \mathbf{L}\phi_s(\mathbf{r},E)\rangle}{\langle \phi_0^\dagger(\mathbf{r},E), \mathbf{P}\phi_s(\mathbf{r},E)\rangle} = 1 + \varphi^* \frac{S}{F}. \tag{16}$$

From Eqs. (8), (12), and (16), the following relation between k_s and k_{eff} can be obtained:

$$\left(1 - \frac{1}{k_{eff}}\right) = \varphi^* \left(1 - \frac{1}{k_s}\right). \tag{17}$$

Finally, the multiplication factors k_s and k_{eff} can be theoretically correlated with the neutron source efficiency φ^*.

For the subcritical system in steady state, k_s is quite a more substantial multiplication factor than k_{eff} since the former is obtained from the balance equation with external source and corresponds to the actual flux of the system.

2.3. Measurement of k_s and φ^* using the reaction rate distribution

QUESTO CAPITOLO E' IL CUORE SCIENTIFICO SPERIMENTALE

Whereas the parameters k_s and φ^* were usually evaluated by numerical calculations in the previous studies (Lebrat et al., 1999; Seltborg and Jacqmin, 2001a, 2001b; Seltborg et al., 2003), a special attention was paid here to examine an experimental method for evaluation of k_s and φ^*.

On the basis of the previous methodology (Shahbunder et al., 2010), k_s can be easily measured by employing the same methodology and using the reaction rate distribution in the subcritical system. According to this methodology, the fission and source neutrons F and S given in Eqs. (9) and (10), respectively, can be approximated and expressed as follows:

$$F \simeq C_{f1} \int_{V_F} \int_0^\infty \Sigma_{D1}(E)\phi_s(\mathbf{r},E)\, dE\, d^3r, \tag{18}$$

$$S \simeq C_{s2} \int_{V_S} \int_0^\infty \Sigma_{D2}(E)\phi_s(\mathbf{r},E)\, dE\, d^3r, \tag{19}$$

where D1 is a detection material having a reasonable cross-section proportionality with the $^{235}U(n,f)$ reaction in the fuel region V_F, D2 is a detection material with a suitable threshold energy for measuring the fast neutrons generated in the target region V_S, and the constants C_{f1} and C_{s2} are assumed to be energy and position independent.

Due to their cross-section characteristics, which satisfy the requirements of detection materials D1 and D2, the $^6Li(n,t)\alpha$ and $^{232}Th(n,f)$ reactions had been employed in the actual measurements of F and S, respectively. By using ^6Li and ^{232}Th detectors, Eqs. (18) and (19), and, approximation of the energy integrated reaction rate of D1 by variable separation (i.e. $R_1(x,y,z) = A_1 R_1(x) R_1(y) R_1(z)$), then k_s in Eq. (8) can be expressed as follows:

$$k_s = \frac{C_{Li}A_{Li}\int_a R_{Li}(x,y_0,z_0)\,dx \int_b R_{Li}(x_0,y,z_0)\,dy \int_c R_{Li}(x_0,y_0,z)\,dz}{C_{Li}A_{Li}\int_a R_{Li}(x,y_0,z_0)\,dx \int_b R_{Li}(x_0,y,z_0)\,dy \int_c R_{Li}(x_0,y_0,z)\,dz + C_{Th}\int_{V_S} R_{Th}(\mathbf{r})\,d^3r}, \tag{20}$$

where C_{Li} is the fission neutrons to the $^6Li(n,t)\alpha$ reaction rate ratio in the subcritical core obtained by calculation, A_{Li} is the constant of the variable separation assumption; $R_{Li}(x,y_0,z_0)$, $R_{Li}(x_0,y,z_0)$ and $R_{Li}(x_0,y_0,z)$ are the energy integrated $^6Li(n,t)$ reaction rate distributions measured in at least one of the x-, y- and z-directions, respectively, in the core with rectangular cuboid geometry whose dimensions are a, b and c; C_{Th} is the source to the $^{232}Th(n,f)$ reaction rate ratio obtained by calculation, and $R_{Th}(\mathbf{r})$ is the energy integrated $^{232}Th(n,f)$ reaction rate measured in the target region.

Finally, by measuring k_s and k_{eff}, the source efficiency φ^* can be easily experimentally evaluated from Eq. (17).

3. Numerical investigation of k_s and φ^*

3.1. Simple subcritical model

A two-dimensional (radius r and height z) model of a simple subcritical core was introduced to examine the effect of subcriticality, source position, and energy on k_s and φ^*, and to investigate the behaviour of the multiplication factors k_s and k_{eff} defined in Section 2.2.

The simple subcritical core is composed of enriched uranium and reflected with light water shown in Fig. 1. The fuel region consists of UO_2F_2 solution with ^{235}U enrichment of 4.89% weight percent and $H/^{235}U$ ratio of 524, placed in a thin Al cylindrical container of 402.4 mm diameter (Paxton and Pruvost, 1986). The UO_2F_2 solution height was adjusted to 382.8 mm to obtain the initial state of $k_{eff} = 0.99837 \pm 0.00003$.

In order to conduct the numerical investigation, well-known external sources were employed, including D–D and D–T reactions, placed at the center of the subcritical core. The calculation model was set up to evaluate k_s and φ^* parameters for the following effects:

(i) *Fuel height change* – The subcriticality was reduced by changing the UO_2F_2 solution height from 382.8 mm down to 0.1 mm in 22 steps. For each step, a 14 MeV point source was always placed at the center of fuel region. The procedures were repeated again with the same source but placed outside the core (r = 402.4 mm), while the source elevation (z) was always aligned with the center of fuel region for consistency.

(ii) *Source position change* – The subcriticality was fixed at 0.97525 in k_{eff} with the UO_2F_2 solution height at 330.0 mm, while the 14 MeV point source position was moved from the center of fuel region to the outer reflector boundary in 11 steps every 50 mm in the r-direction.

(iii) *Source energy change* – The subcriticality was fixed for two states whose k_{eff} was 0.95 and 0.98 by setting a suitable UO_2F_2 solution height. For each state, the point source position was fixed at the center of fuel region, while the source energy was varied from 1 to 14 MeV in four steps.

For each step in above, k_s and φ^* were calculated using Eqs. (8) and (17), respectively, where the quantities of F, S and k_{eff} were obtained from standard MCNPX (Pelowitz, 2005) outputs with ENDF/B-VI.8 (Rose, 1991).

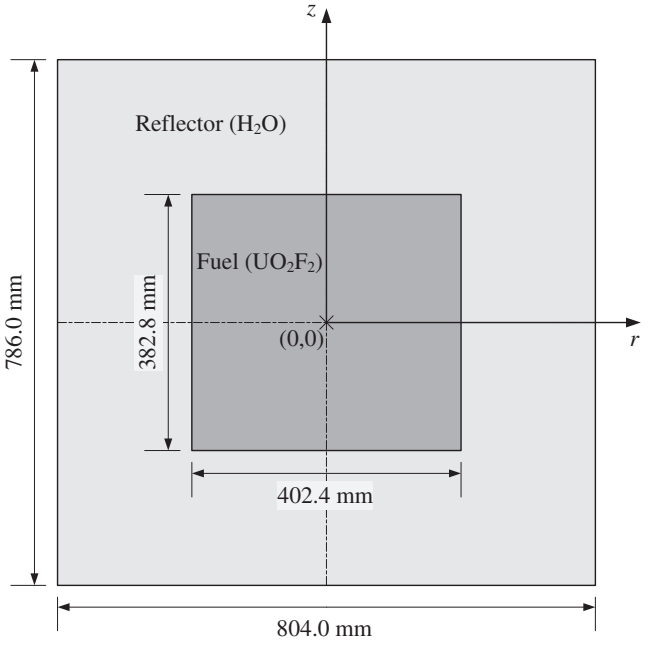

Fig. 1. Side view of the calculation model of a reflected cylindrical reactor in initial state of k_{eff} = 0.99837.

3.2. Numerical calculations

3.2.1. Effect of subcriticality

The subcriticality change in the system had covered a wide range of 0.01507–0.99837 in k_{eff} with standard deviation of 0.00007 in average by MCNPX. The following discussion focuses on the effect of subcriticality (in case of inside and outside core source) on two parameters, namely, the discrepancy between k_s and k_{eff}, and the average value of φ^*.

For the subcritical states ($k_{eff} \geqslant 0.90$), when the source was placed inside the core, as shown in Fig. 2 and Table 1, k_s was found very close to k_{eff} with a relative difference of less than 1.8%. The φ^* was around 0.9417 and showed the given dependence on k_{eff}. These results indicated that the closer the system is to the critical state, the more the relative values of ϕ_s and ϕ_0 become approximately equal each other, and so do the values of k_s and k_{eff}.

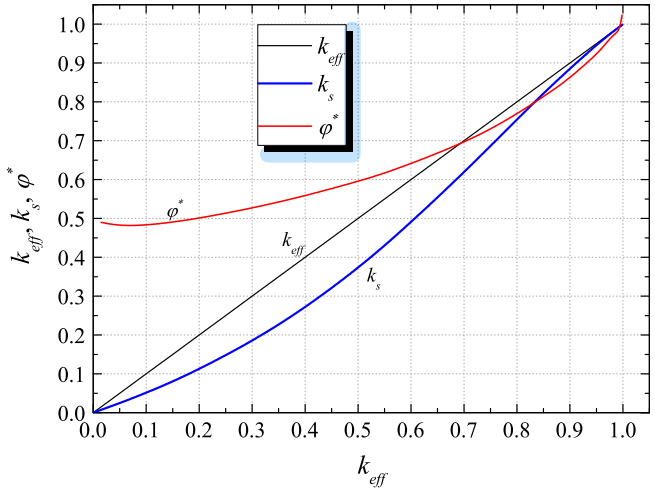

Fig. 2. Effect of subcriticality on subcritical multiplication factor k_s and source efficiency φ^* for a fixed source inside the fuel region.

Table 1
Summary of subcriticality effect on k_s and φ^* for a 14 MeV source in the simple subcritical model.

k_{eff}	Source position	$(k_s/k_{eff} - 1)_{max}$ (%)	φ^* (average)
⩾0.90	Inside core	−1.8	0.9417
	Outside core	−75	0.0388
<0.90	Inside core	−50.6	0.5939
	Outside core	−98.0	0.0232

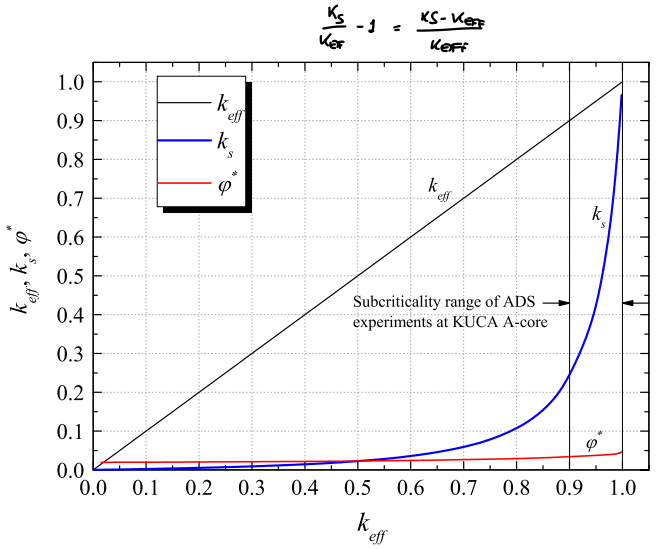

Fig. 3. Effect of subcriticality on subcritical multiplication factor k_s and source efficiency φ^* for a fixed source outside the core.

Inversely, when the source was placed outside the core and for the same range ($k_{eff} \geqslant 0.90$), the discrepancy between k_s and k_{eff} became much larger as the maximum relative difference was 75%, as shown in Fig. 3 and Table 1. While the magnitude of φ^* was considerably reduced to around 0.0388, it showed higher dependence on k_{eff} (i.e. higher φ^* maximum to minimum ratio) compared to the inside source case at the same range ($k_{eff} \geqslant 0.90$). The relative higher divergence of k_s and k_{eff}, found even in the close to critical states in this case, was attributed to the source existence outside the core.

For the deeper subcritical states ($k_{eff} \leqslant 0.90$), regardless of the source position, the discrepancy between k_s and k_{eff} was further increased as shown in Figs. 2 and 3, and Table 1, since the neutron leakage effects increased according to changing the size of fuel region.

3.2.2. Effect of source position

The effect of changing the source position along the r-axis for a fixed moderate subcritical state as above (k_{eff} = 0.975) is shown in Fig. 4. The results showed the exact variation of the source efficiency at different positions, and indicated that the highest source efficiency was achieved when the source is placed at the center of the core. This fact revealed the possibility of using φ^* in evaluating the best source position precisely for more complex systems, where the geometric center of the core should not necessarily correspond to the source position producing the maximum efficiency.

3.2.3. Effect of source energy

As shown in Table 2, for two states of k_{eff} (0.95 and 0.98) with the source placed inside the core, the lower energy sources of 1 and 2.45 MeV produced φ^* of higher than 1.57, and k_s was consequently higher than k_{eff}. Conversely, the higher energy sources of 10 and 14 MeV produced lower φ^* from 0.93 to 1.04, and k_s lower

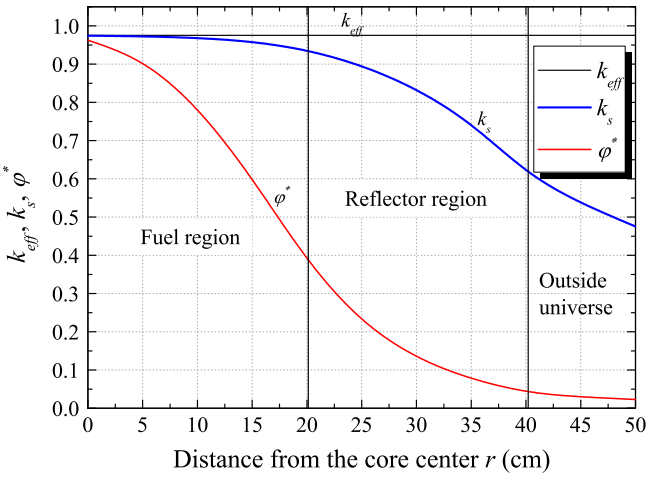

Fig. 4. Effect of source position on subcritical multiplication factor k_s and source efficiency φ^* for a fixed subcritical state of k_{eff} = 0.975.

Table 2
Effect of source energy on k_s and φ^* for a source at the core center in the simple subcritical model.

Source (MeV)	k_{eff} = 0.950 ± 0.001		k_{eff} = 0.980 ± 0.001	
	k_s[a]	φ^*[b]	k_s[a]	φ^*[b]
1	0.974	1.95	0.990	1.98
2.45	0.968	1.57	0.988	1.62
10	0.950	0.99	0.981	1.04
14	0.946	0.93	0.979	0.97

[a] Statistical error in k_s is less than 0.001.
[b] Statistical error in φ^* is less than 0.01.

than k_{eff}. These results indicated that the lower energy source neutrons are more effective in the simple subcritical model of the thermal spectrum. This phenomena could be linked to the lower probability of leakage of the lower energy source neutrons, which means higher ability to contribute to the neutron production. Additionally, it could be easier for the moderator to "shift" the lower, rather than higher, energy source spectrum into the thermal region where the fission cross-section is larger for the given ^{235}U fuel.

Further, an increase of φ^* to higher than unity demonstrated that the average source neutron importance could become higher than the average fission neutron importance according to the source efficiency definition. This phenomena was observed here (e.g., 1 and 2.45 MeV in Table 2, k_{eff} higher than 0.99 in Fig. 2), because the source neutrons emitted exclusively from the center of fuel region had lower chances to escape from the core than the average fission neutrons and, as a result, the higher importance.

The numerical investigation using the simple subcritical model in this section demonstrated k_s and φ^* behaviour in details and indicated the importance of their evaluation in ADS for optimizing the subcritical system, source position and energy.

4. ADS experiments

4.1. Description of the KUCA A-core

The KUCA A-core is composed of a highly-enriched uranium, solid-moderated and -reflected with polyethylene shown in Fig. 5, and coupled with an external 14 MeV pulsed neutron generator. The standard fuel rod "F" is composed of 36 times of 2″ square fuel unit of 93% enriched uranium–aluminum alloy plate 1/16″ thick combined with polyethylene plates 1/8″ and 1/4″ thick in addition to an upper and lower polyethylene blocks 591 and 537 mm

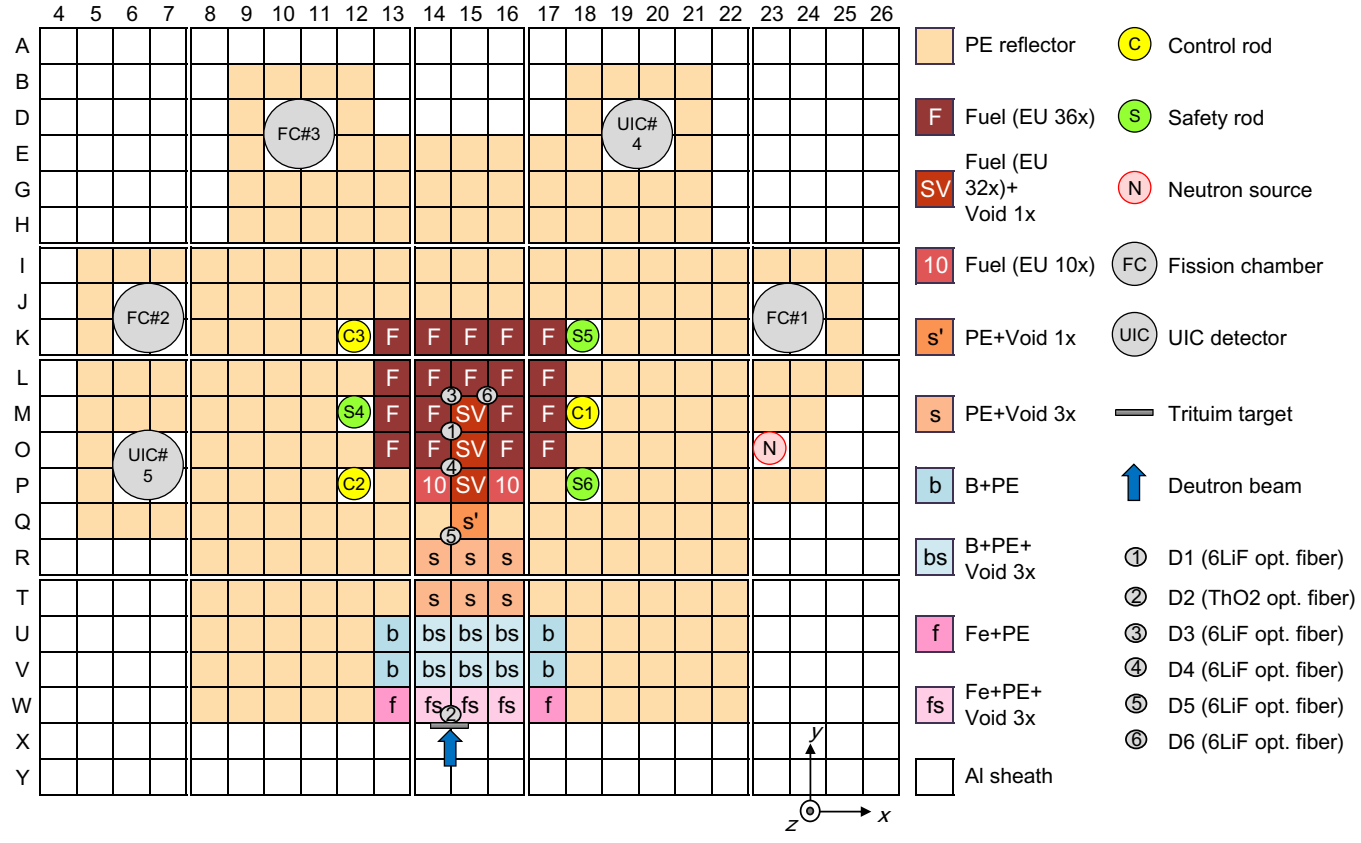

Fig. 5. Top view of A-core configuration with a neutron guide and a beam duct.

length, respectively. The fuel rod "10" corresponds to a standard fuel rod but with 10 fuel units. The "SV" fuel rod is composed of 32 fuel units and a cubic void of 50 mm side length in the center of the fuel region. The tritium target of the pulsed neutron generator is located outside the core. Here, the "SV" fuel assembly with the void and a neutron guide (Pyeon et al., 2007) were installed in the fuel and reflector regions, respectively, for directing the highest number of the neutrons from the target to the core center. The neutron guide is composed of several shielding materials, including iron, boron, polyethylene and the beam duct (Pyeon et al., 2007, 2008, 2009a).

4.2. Experiments and calculations

On the basis of the numerical investigation in Section 3.2, the ADS experiments were carried out at the KUCA A-core, shown in Fig. 5, to experimentally evaluate k_s and φ^* by using the measured reaction rate distribution. The critical state was experimentally achieved by the withdrawal of all control and safety rods except for control rod (C3) being partially inserted. Nine cases of subcritical states were considered where the subcritical system was varied according to the insertion pattern of the control and safety rods and/or reducing the number of applied "F" fuel rods as shown in Table 3. The base configuration has included 18 fuels rods as shown in Fig. 5 (Cases 1 and 2), then they were reduced to 16 (Cases 3–5) by removing "F" at the positions (O, 13) and (O, 17), then reduced to 14 (Cases 6–8) by removing "F" at the positions (M, 13) and (M, 17), and finally reduced to 12 (Case 9) by removing "F" at the positions (L, 13) and (L, 17). The removed fuel rods were always replaced by PE reflector.

Table 3
Subcritical states of the ADS experiments at the KUCA A-core.

Case	Number of fuel rods	Rods insertion
Critical state	18	C3 (partially)
1	18	C1, C2, C3
2	18	C1, C2, C3; S4, S5, S6
3	16	No insertion
4	16	C1, C2, C3
5	16	C1, C2, C3; S4, S5, S6
6	14	No insertion
7	14	C1, C2, C3
8	14	C1, C2, C3; S4, S5, S6
9	12	No insertion

Table 4
Comparison between measured k_{eff} by pulsed neutron method using four ^{6}LiF optical fiber detectors (D3–D6) in the KUCA A-core experiments.

Case	Optical fiber D3	Optical fiber D4	Optical fiber D5	Optical fiber D6
1	0.9902 ± 0.0001	0.9905 ± 0.0001	0.9902 ± 0.0001	0.9907 ± 0.0001
2	0.9816 ± 0.0002	0.9790 ± 0.0002	0.9825 ± 0.0002	0.9824 ± 0.0002
3	0.9752 ± 0.0002	0.9697 ± 0.0003	0.9764 ± 0.0002	0.9766 ± 0.0002
4	0.9671 ± 0.0003	0.9686 ± 0.0003	0.9650 ± 0.0003	0.9713 ± 0.0003
5	0.9571 ± 0.0004	0.9615 ± 0.0004	0.9560 ± 0.0004	0.9643 ± 0.0003
6	0.9444 ± 0.0005	0.9386 ± 0.0006	0.9357 ± 0.0006	0.9559 ± 0.0004
7	0.9381 ± 0.0006	0.9090 ± 0.0008	0.9297 ± 0.0007	0.9532 ± 0.0004
8	0.9298 ± 0.0006	0.9190 ± 0.0007	0.9205 ± 0.0007	0.9521 ± 0.0005
9	0.9071 ± 0.0008	0.8907 ± 0.0010	0.8934 ± 0.0009	0.9341 ± 0.0006

The reaction rate distributions in the subcritical states were measured in the z-direction from the center of the core to the reflector region, for Cases 1–9, by using a movable optical fiber detector (D1) (Mori et al., 1994; Yagi et al., 2008) inserted in a small gap between the assemblies at the position of (M–O, 14–15) in Fig. 5. The optical fiber was composed of a powder mixture of ^{6}Li enriched LiF converter and ZnS(Ag) scintillator pasted on one end of a plastic optical fiber 1 mm diameter with an instant adhesive. Another $^{232}ThO_2$ fiber (D2) was set in front of the tritium target, and fixed to obtain the source neutron information. Subcriticality of nine cases was measured using the pulsed neutron method with optical fiber detectors (D3, D4, D5, D6) placed in the core in the positions shown in Fig. 5. The prompt neutron decay constant used to deduce the subcriticality was obtained by the extrapolated area ratio method (Gozani, 1962).

Eigenvalue calculations were executed by MCNPX with ENDF/B-VI.8 to obtain k_{eff} for the nine cases. The active cycle of histories used in the eigenvalue calculations was 4×10^7 with standard deviation 0.00013. The fixed source calculations were executed for the nine cases at the subcritical states to obtain the ^{6}Li(n, t) reaction rate distribution in the fuel region as follows: the z-direction from the center of the core to the reflector region at the position (M–O, 14–15); the x-direction from the position (M–O, 14–15) until (M–O, 17–18); the y-direction from the position (M–O, 14–15) until (K–J, 14–15). The calculations have also included the ^{232}Th(n, f) reaction rate in the target region and the total fission and source neutrons. The number of histories used in the fixed source calculations was 1×10^8 and the statistical error was 1.4%.

4.3. Results and discussion

The effective multiplication factor k_{eff} of the nine cases measured by each of the four optical fiber detectors (D3–D6) is shown in Table 4. The slight increase in the variation of the detectors mea-

Table 5
Comparison between measured and calculated k_{eff}, k_s and φ^* in the KUCA A-core experiments.

Case	k_{eff}		k_s		φ^*	
	Exp.[a]	Cal.[b]	Exp.[c]	Cal.[d]	Exp.[e]	Cal.[f]
1	0.9904 ± 0.0002	0.9909 ± 0.0001	0.7770 ± 0.0259	0.7104 ± 0.0012	0.034 ± 0.005	0.022 ± 0.000
2	0.9814 ± 0.0014	0.9824 ± 0.0001	0.4377 ± 0.0374	0.5521 ± 0.0010	0.015 ± 0.003	0.022 ± 0.000
3	0.9744 ± 0.0028	0.9760 ± 0.0001	0.4422 ± 0.0389	0.4538 ± 0.0009	0.021 ± 0.004	0.020 ± 0.000
4	0.9680 ± 0.0023	0.9681 ± 0.0001	0.3750 ± 0.0383	0.3778 ± 0.0008	0.020 ± 0.004	0.020 ± 0.000
5	0.9597 ± 0.0033	0.9611 ± 0.0001	0.3266 ± 0.0369	0.3266 ± 0.0006	0.020 ± 0.004	0.020 ± 0.000
6	0.9436 ± 0.0076	0.9421 ± 0.0001	0.2393 ± 0.0317	0.2424 ± 0.0004	0.019 ± 0.004	0.020 ± 0.000
7	0.9322 ± 0.0158	0.9369 ± 0.0001	0.2184 ± 0.0302	0.2230 ± 0.0004	0.020 ± 0.006	0.019 ± 0.000
8	0.9302 ± 0.0129	0.9323 ± 0.0001	0.2241 ± 0.0313	0.2085 ± 0.0004	0.022 ± 0.006	0.019 ± 0.000
9	0.9060 ± 0.0166	0.9076 ± 0.0001	0.2021 ± 0.0304	0.1600 ± 0.0003	0.026 ± 0.007	0.019 ± 0.000

[a] Pulsed neutron method.
[b] Eigenvalue calculations.
[c] Reaction rate distribution (3-dimesnional) and Eq. (20).
[d] Eq. (8), calculated F and S.
[e] Eq. (17), measured k_s and k_{eff}.
[f] Eq. (17), calculated k_s and k_{eff} (actual error in cal. φ^* was less than 1.5%).

Table 6
Relative difference in measured and calculated k_{eff}, k_s and φ^*.

Case	$(C/E-1)$ (%)		
	k_{eff}	k_s	φ^*
1	0.1 ± 0.0	−8.6 ± 0.3	−33.4 ± 5.1
2	0.1 ± 0.0	26.1 ± 2.2	49.8 ± 8.5
3	0.2 ± 0.0	2.6 ± 0.2	−1.9 ± 0.4
4	0.0 ± 0.0	0.8 ± 0.1	0.9 ± 0.2
5	0.1 ± 0.0	0.0 ± 0.0	−3.6 ± 0.7
6	−0.2 ± 0.0	1.3 ± 0.2	4.7 ± 1.1
7	0.5 ± 0.0	2.1 ± 0.3	−4.8 ± 1.5
8	0.2 ± 0.0	−6.9 ± 1.0	−11.8 ± 3.2
9	0.2 ± 0.0	−20.8 ± 3.1	−26.2 ± 7.1

surements when subcriticality was increased, was attributed to the different detector positions (the fuel and reflector regions), specially in the deeper subcritical states. A more extensive discussion of the measured subcriticalities of these experiments, including the reaction rate time distribution, the prompt neutron decay constant, and the delayed neutron fraction, is presented in detail in the kinetic analysis of a previous study (Pyeon et al., 2008).

The final measured k_{eff} of each case was estimated by the average values of the four detectors (D3–D6). As shown in Table 5, a comparison between the measured and calculated k_{eff} of the nine cases revealed fairly good agreement within a maximum relative difference 0.5% as shown in Table 6. These results demonstrated the good precision of MCNPX with ENDF/B-VI.8 in eigenvalue calculations in various control/safety rods configurations, and was one way for the validation of the calculation model prior to the fixed source calculations to obtain the reaction rate distributions and the total fission rate in the subcritical system.

The measured reaction rate distribution in the z-direction by the LiF optical fiber detector (D1) was finely reproduced with MCNPX specially in the shallow subcritical states and the fuel region. A representation of the measured and calculated reaction rate distribution relative to the calculation for Cases 1, 2 and 5 is shown in Fig. 6. Since the reaction rate distribution was measured only in the z-direction, it was necessary to calculate the x- and y-distribution in order to examine the objective k_s parameter using the 3-dimenional reaction rate profile as required by Eq. (20).

The fission neutrons to the ^{6}Li$(n,t)\alpha$ reaction rate ratio C_{Li} was obtained by calculation and examined in four possibilities of the

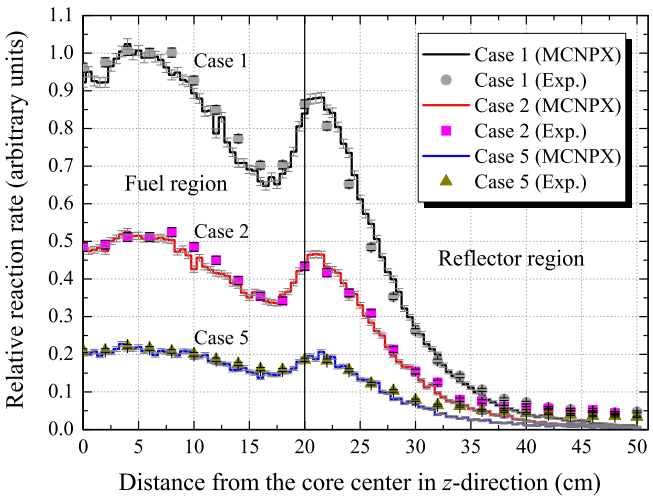

Fig. 6. Comparison between the relative measured and calculated reaction rate distribution for Cases 1, 2, and 5.

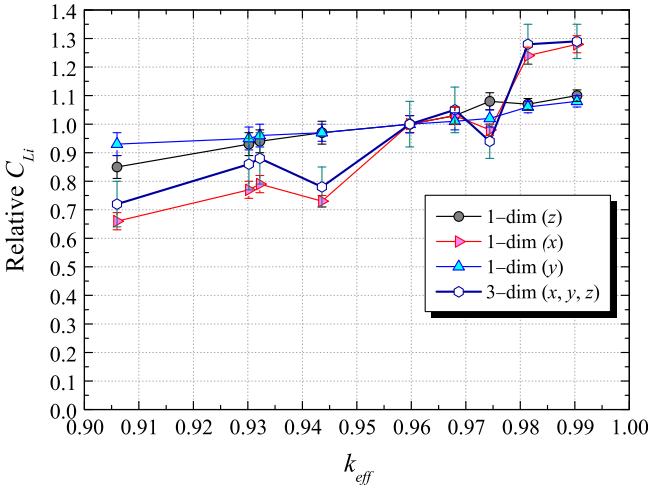

Fig. 7. Comparison between C_{Li} (fission neutrons to ^{6}Li$(n,t)\alpha$ reaction rate ratio) obtained by MCNPX calculation with 1-dimensional and 3-dimensional dependence of reaction rate approximation by variable separation.

energy integrated ^{6}Li$(n,t)\alpha$ reaction rate function $R_{\mathrm{Li}}(x,y,z)$ variable separation, three of which assuming one-dimensional dependence, i.e. $R_{\mathrm{Li}}(x,y,z) = A_{\mathrm{Li}}R_{\mathrm{Li}}(x,y_0,z_0)$; $R_{\mathrm{Li}}(x,y,z) = A_{\mathrm{Li}}R_{\mathrm{Li}}(x_0,y,z_0)$; $R_{\mathrm{Li}}(x,y,z) = A_{\mathrm{Li}}R_{\mathrm{Li}}(x_0,y_0,z)$, and the fourth assuming the three-dimensional dependence as has been actually used in Section 2.3 and Eq. (20), i.e. $R_{\mathrm{Li}}(x,y,z) = A_{\mathrm{Li}}R_{\mathrm{Li}}(x,y_0,z_0)R_{\mathrm{Li}}(x_0,y,z_0)R_{\mathrm{Li}}(x_0,y_0,z)$. The feasibility of the 3-dimensional analysis and the validity of using the C_{Li} for the fission neutrons F approximation, used in Eq. (18), can be examined from the comparison between the above four assumptions effect on the variation of C_{Li} values in all measured k_{eff} as shown in Fig. 7.

The 1-dimensional dependence in the y- and z-directions was found the best of approximations as the variation in C_{Li} was minimized in these cases. However, the 1-dimensional dependence in the x-direction was found to increase C_{Li} variation in effect to the local perturbation on the reaction rate distribution in this direction caused by the control rod "C1" and fuel rods "F" at positions (O:M, 17) insertion/withdrawal patterns among some of the configurations, that was in direct vicinity to the calculated reaction rate in the x-direction in this region. Employing the 3-dimensional dependence was significantly affected by the increased C_{Li} variation in case of the x-dimension, and thus could not fairly confirm the advantage of the 3-dimensional over the 1-dimensional analysis in these experiments. However, since the 3-dimensional analysis resulted at least in lower C_{Li} variation than the worst case of the 1-dimensional analysis, namely the x-direction, the advantage of the 3-dimensional analysis could be confirmed when the dimensional dependence effect of each direction on the reaction rate approximation is not exactly well known before carrying out the actual experiments or calculations. By evaluation of the C_{Li} coefficient (using calculation) and the ^{6}Li$(n,t)\alpha$ reaction rate distribution (using experimental z-profile measured by "D1" and calculational x- and y-profiles), the fission neutrons F in the core could be obtained as given by Eq. (18).

The calculated ^{232}Th(n,f) reaction rate in front of the target region did not show any variation in the MCNPX calculation of all cases which caused the coefficient C_{Th} to remain unchanged according to Eq. (19), while some variation was observed in the measurements using the ThO_2 optical fiber detector (D2) according to the possible variation in the source intensity. Thus the source intensity could be experimentally evaluated using Eq. (19) with C_{Th} (by calculation) and the integrated reaction rate (by experiment from the ThO_2 optical fiber detector "D2").

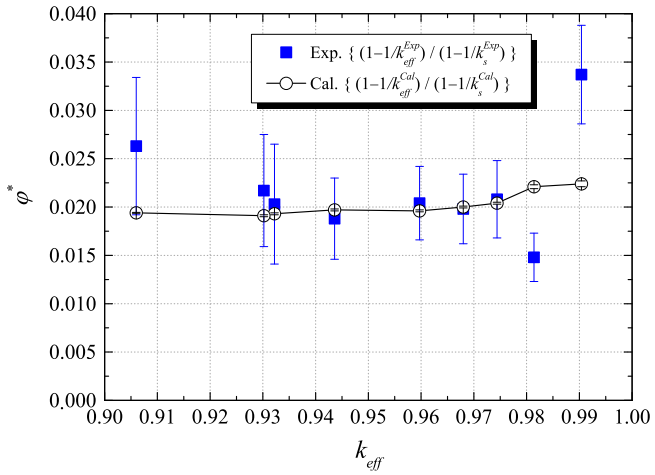

Fig. 8. Comparison between the measured and calculated source efficiency φ^* versus the measured k_{eff}.

4.3.1. Subcritical multiplication factor k_s

The measured k_s was obtained using Eq. (20), and the reaction rate distribution based on the 3-dimensional analysis, such that the z-direction as measured by the optical fiber detector (D1) and the x- and y-directions as calculated by MCNPX. The C_{Li} coefficient, in Eq. (18), of Case 5 was obtained by calculation and used in evaluating k_s in all cases, since this coefficient was closest to the average value in any subcritical states as shown in Fig. 7. The calculated k_s was obtained using Eq. (8) with calculated F and S in Eqs. (9) and (10), respectively.

As shown in Table 5, for the given range ($k_{eff} > 0.90$), k_s was found smaller than k_{eff} in all cases in which the maximum relative difference was around 80%. This behaviour was confirmed in the simple subcritical model results discussed in Section 3.2, since a maximum relative difference of 75% between k_s and k_{eff} was observed, as shown in Table 1, for the same conditions regarding the k_{eff} range and using 14 MeV source outside the fuel region. Based on the important perspective obtained in Section 3.2, the serious discrepancy between the measured k_s and k_{eff} found in Table 5 was also attributed to the existence of 14 MeV neutron source outside the A-core.

Furthermore, the comparison between measured and calculated k_s, as shown in Table 5, revealed fairly good agreement within a relative difference of 6.9% in most of the cases while larger in the others, as shown in Table 6. The main reasons of inducing the discrepancy between the measured and calculated k_s were, on the one hand, the differences observed in the actual calculated C_{Li} values compared to Case 5, specially in Cases 1, 2 and 9 as shown in Fig. 7, and on the other hand, the difficulty to guarantee the exact absolute values of the optical fibers count rates used to measure the reaction rate, since the amount ($\sim 10^{-3}$ g) of the converter and scintillator pasted on the fibers could not be made exactly identical in all cases. These results indicated, to some extent, the applicability of measurement of k_s in Eq. (20) using the reaction rate distribution.

Additionally, once k_s is determined, it is easy to evaluate the relative value of the reactor power, since it can be seen proportional to the ratio $k_s/(1\text{-}k_s)$ as given in Eq. (2).

4.3.2. Source efficiency φ^*

The experimental φ^* was obtained using Eq. (17) with both measured k_{eff} and k_s by the pulsed neutron method and Eq. (20), respectively. The calculated φ^* was also obtained using Eq. (17) but with both calculated k_{eff} and k_s.

The results of φ^* in Table 5 showed some dependence of subcriticality for the given range of ($k_{eff} > 0.90$), since it was found slightly changing at a value of around (0.0215 ± 0.0012) – quite low due to the existence of the source outside the core region. In other words, an outer source contributed to the "escape" of some source neutrons before their actual penetration inside the core, and thus significantly reduced the source efficiency magnitude for the given system. The magnitude of φ^* was found of the same order as that in the case of the simple subcritical model, where also the change in φ^* was maintaining a close behaviour, under the same conditions of k_{eff} and source position and energy, as shown in Fig. 3 and Table 1.

The comparison between the measured and calculated φ^*, shown in Table 5, was observed within a relative difference ($C/E - 1$) of nearly the same behaviour of that of k_s as it was less than 11.8% in most of the cases while much larger in the others as given in Table 6. The reason of this discrepancy is attributed to the difference in the measured and calculated k_s itself, described in the previous section, in addition to the difference in the measured and calculated k_{eff}. Further representation for the behaviour of the measured and calculated φ^* in various k_{eff}, seen in Fig. 8, shows the relative difference could be accepted in view of the low values of φ^* and the given statistical error.

Despite some degree of discrepancy in measurement and calculation, the source efficiency φ^* was successfully measured by experiment to a certain precision, that could be improved by employing a more accurate expansion rather than the variable separation of the reaction rate in the subcritical system, and moreover, confirming the exact consistency of the absolute count rates used to measure the reaction rate in the various configurations.

5. Conclusion

An experimental methodology to evaluate the subcritical multiplication factor k_s and the neutron source efficiency φ^* was proposed by using the reaction rate distribution. Prior to the actual experiments, the numerical investigation using a simple model of a thermal subcritical reactor demonstrated the dependence of k_s and φ^* on subcriticality, source position, and energy.

On the basis of the theoretical and numerical preparations, k_s and φ^* were experimentally evaluated through a series of ADS experiments with 14 MeV neutrons by using the measured reaction rate distribution in the subcritical system, within a relative difference between the measured and calculated values of less than 7% and 12% for k_s and φ^*, respectively, in most cases.

Further investigation of the ADS parameters, including k_s and φ^*, could be conducted to examine the feasibility of experimental methodology using the reaction rate distribution for another external neutron source, such as a spallation source from a high-energy protons beam and a heavy metal target.

References

Carminati, F. et al., 1993. An Energy Amplifier for Cleaner and Inexhaustible Nuclear Energy Production Driven by a Particle Beam Accelerator. CERN-AT-93-47-ET.

Delpech, M. et al., 1999. The Am and Cm transmutation-physics and feasibility. In: Proceedings of the International Conference on Future Nuclear Systems, Wyoming, USA, August 30–September 2, 1999. ANS, Jackson Hole.

Duderstadt, J.J., Hamilton, L.J., 1976. Nuclear Reactor Analysis. John Wiley & Sons, NY, USA.

Gandini, A., Salvatores, M., 2002. The physics of subcritical multiplying systems. Journal of Nuclear Science and Technology 39 (6), 673–686.

Gozani, T., 1962. A modified procedure for the evaluation of pulsed source experiments in subcritical reactors. Nukleonik 4, 348.

Heuer, D. et al., 1997. Proposal for an accelerator driven subcritical reactor pilot unit. In: Proceedings of the International Conference on Future Nuclear Systems, GLOBAL'97, Yokohama, Japan, September 5–10, 1997, p. 440.

Kiyavitskaya, H., 2007. Yalina Subcritical Facility to Investigate Neutronics of ADS: Yalina-thermal Benchmark, Yalina-booster Benchmark. IAEA Technical Meeting, Rome, Italy, 12–16 November 2007.

Kobayashi, K., Nishihara, K., 2000. Definition of subcriticality using the importance function for the production of fission neutrons. Nuclear Science and Engineering 136 (2), 272–281.

Lebrat, J.F. et al., 1999. Experimental investigation of multiplying subcritical media in presence of an external source operating in pulsed or continuous mode: the MUSE-3 experiment. In: Proceedings of the 3rd International Conference on Accelerator-Driven Transmutation Technologies and Applications, Prague, Pruhonice, Czech Rep., June 7–11, 1999.

Misawa, T., Unesaki, H., 2003. Measurement of subcriticality by higher mode source multiplication method. In: Proceedings of the 7th International Conference on Nuclear Criticality Safety, ICNC'03, Tokai-mura, Japan, October 20–24, 2003.

Mori, C. et al., 1994. Simple and quick measurement of neutron flux distribution by using an optical fiber with scintillator. Journal of Nuclear Science and Technology 31 (3), 248–249.

Nishihara, K., Iwasaki, T., Udagawa, Y., 2003. A new static and dynamic one-point equation and analytic and numerical calculations for a subcritical system. Journal of Nuclear Science and Technology 40 (7), 481–492.

Paxton, H.C., Pruvost, N.L., 1986. Critical Dimensions of Systems Containing U-235, Pu-239 and U-233. Technical Report, LA-10860, Los Alamos National Labortaory, New Mexico [Revision of June 1964 Report].

Pelowitz, D.B., 2005. MCNPX User's Manual Version 2.5.0. LANL Report, LA-CP-05-0369, Los Alamos National Laboratory.

Persson, C.M. et al., 2005. Analysis of reactivity determination methods in the subcritical experiment Yalina. Nuclear Instruments and Methods in Physics Research A 554, 374–383.

Persson, C.M. et al., 2008. Pulsed neutron source measurements in the subcritical ADS experiment Yalina-booster. Annals of Nuclear Energy 35 (12), 2357–2364.

Pyeon, C.H. et al., 2007. Preliminary experiments on accelerator-driven subcritical reactor with pulsed neutron generator in Kyoto University Critical Assembly. Journal of Nuclear Science and Technology 44 (11), 1368–1378.

Pyeon, C.H. et al., 2008. Static and kinetic experiments on accelerator-driven system with 14 MeV neutrons in Kyoto University Critical Assembly. Journal of Nuclear Science and Technology 45 (11), 1171–1182.

Pyeon, C.H. et al., 2009a. Reaction rate analysis for an accelerator-driven system with 14 MeV neutrons in the Kyoto University Critical Assembly. Journal of Nuclear Science and Technology 46 (10), 965–972.

Pyeon, C.H. et al., 2009b. First injection of spallation neutrons generated by high-energy protons into the Kyoto University Critical Assembly. Journal of Nuclear Science and Technology 46 (12), 1091–1093.

Rose, P.F., 1991. ENDF-201, ENDF/B-VI Summary Documentation. fourth ed., National Nuclear Data Center. BNL-NCS-17541.

Salvatores, M., 1999. Accelerator driven systems (ADS), physics principles and specificities. Journal de Physique IV 9 (PR7), 7-17–7-33.

Seltborg, P., Jacqmin, R., 2001a. Investigation of neutron source effects in sub-critical media and application to a model of the MUSE-4 experiments. In: Proceedings of International Meeting on Mathematical Methods for Nuclear Applications, Salt Lake, USA, September 9–13, 2001. ANS.

Seltborg, P., Jacqmin, R., 2001b. Spallation neutron source effects in a sub-critical system. In: Proceedings of International Topical Meeting on Accelerator Applications/Accelerator Driven Transmutation Technology Applications, Reno, NV, USA, November 11–15, 2001. ANS.

Seltborg, P., Wallenius, J., Tuček, K., Gudowski, W., 2003. Definition and application of proton source efficiency in accelerator-driven systems. Nuclear Science and Engineering 145 (3), 390–399.

Shahbunder, H., Pyeon, C.H., Misawa, T., Shiroya, S., 2010. Experimental analysis for neutron multiplication by using reaction rate distribution in accelerator-driven system. Annals of Nuclear Energy 37 (4), 592–597.

Shi, Y.Q., Zhu, Q.F., Tao, H., 2005. Review and research of the neutron source multiplication method in nuclear critical safety. Nuclear Technology 149 (1), 122–127.

Shiroya, S. et al., 2000. Accelerator driven subcritical system as a future neutron source in Kyoto University Research Reactor Institute (KURRI)-basic study on neutron multiplication in the accelerator driven subcritical reactor. Progress in Nuclear Energy 37 (1–4), 357–362.

Takahashi, H., 1994. The Safe, Economical Operation of a Slightly Subcritical Reactor and Transmutor with a Small Proton Accelerator. BNL-60095.

Tanigaki, M. et al., 2006. Present status of FFAG accelerators in KURRI for ADS study. In: Proceedings of the 10th European Particle Accelerator Conference, EPAC'06, Edinburgh, Scotland, June 26–30, 2006.

Yagi, T. et al., 2008. Development of optical fiber detector for measurement of fast neutron. In: Proceeding of the International Conference on the Physics of Reactors, PHYSOR'08, Interlaken, Switzerland, September 14–19, 2008 (CD-ROM).